UMYU Scientifica, Vol. 5 NO. 1, March 2026, Pp 267 – 275
https://doi.org/10.56919/usci.2651.022
ISSN: 2955 – 1145 (print); 2955 – 1153 (online)
A periodical of the Faculty of Natural and Applied Sciences, UMYU, Katsina

ORIGINAL RESEARCH ARTICLE

Ferroelectric-Driven Charge Separation and Cobalt-Induced Defect Engineering in $BaTiO_3$/Co–ZnO Heterostructures for Efficient Visible-Light Photocatalysis

Danasabe Abdullahi Ibrahim[1,2]*, Adam Usman[2] and Ahmed D. Abubakar[2]
[1]Department of Physics, Nigerian Army University, Biu, Nigeria
[2]Department of Physics, Modibbo Adama University, Yola, Nigeria

ABSTRACT
The development of efficient visible-light-driven photocatalysts remains critical for sustainable environmental remediation. In this study, a $BaTiO_3$/Co–ZnO heterostructure (S3) was investigated for the photocatalytic degradation of organic dyes under visible-light irradiation. Structural analysis based on simulated X-ray diffraction (XRD) patterns confirmed the successful formation of a composite system comprising perovskite $BaTiO_3$ and hexagonal Co–ZnO phases. Optical characterization using the Tauc method revealed a reduced bandgap of approximately 2.65 eV, indicating enhanced visible-light absorption compared to pristine ZnO. The photocatalytic performance of the S3 heterostructure was evaluated using crystal violet (CV), methylene blue (MB), and rhodamine B (RhB) as model pollutants. UV–Vis absorption spectra showed a progressive decrease in the characteristic absorption peaks, confirming efficient degradation. After 75 min of irradiation, degradation efficiencies of 99% (CV), 98% (MB), and 99% (RhB) were achieved, outperforming many previously reported ZnO-based photocatalysts. The degradation process followed pseudo-first-order kinetics with rate constants of 0.01775 min^{-1} (CV), 0.02047 min^{-1} (MB), and 0.01992 min^{-1} (RhB) and strong correlation coefficients (R^2 = 0.927–0.983). The enhanced photocatalytic activity is attributed to the synergistic effects of ferroelectric polarization from $BaTiO_3$ and cobalt-induced defect states in ZnO, which facilitate efficient charge separation, suppress electron–hole recombination, and improve interfacial charge transfer. The internal polarization field promotes directional carrier migration, while defect states extend light absorption into the visible region. Reactive oxygen species, including superoxide (O_2•$^-$) and hydroxyl radicals (•OH), play a dominant role in the degradation process. Overall, the $BaTiO_3$/Co–ZnO heterostructure demonstrates a highly efficient and robust photocatalytic system, highlighting the effectiveness of combining ferroelectric materials with defect-engineered semiconductors as a promising strategy for advanced environmental remediation.

ARTICLE HISTORY
Received December 03, 2025
Accepted March 25, 2026
Published March 26, 2026

KEYWORDS
$BaTiO_3$/Co–ZnO heterostructure; Visible-light photocatalysis; Ferroelectric polarization; Defect engineering; Dye degradation; Charge separation

© The Author(s). This is an Open Access article distributed under the terms of the Creative Commons Attribution 4.0 License creativecommons.org

INTRODUCTION
The continuous release of organic pollutants, particularly synthetic dyes and pharmaceutical residues, into water systems has become a critical environmental challenge due to their high stability, toxicity, and resistance to conventional treatment techniques (Chong et al., 2010; Low et al., 2017). These contaminants are often non-biodegradable and can accumulate in aquatic environments, posing significant risks to ecosystems and human health (Ramesh and Spaldin, 2007). Consequently, the development of efficient, sustainable, and cost-effective remediation technologies remains a priority in environmental research.

Semiconductor-based photocatalysis has emerged as one of the most promising advanced oxidation processes due to its ability to utilize solar energy for the degradation of organic pollutants into environmentally benign products such as CO_2 and H_2O (Chen and Mao, 2007; Low et al., 2017). Upon irradiation with photons of sufficient energy, electrons are excited from the valence band to the conduction band of the semiconductor, leaving behind holes. These photogenerated charge carriers participate in redox reactions that produce reactive oxygen species (ROS), including hydroxyl radicals (•OH) and superoxide radicals (O_2•$^-$), which are highly effective in degrading complex organic molecules (Low et al., 2017).

Despite these advantages, conventional semiconductor photocatalysts such as ZnO and TiO_2 suffer from inherent limitations, including rapid recombination of electron–hole pairs and wide bandgap energies that restrict their photoresponse primarily to the ultraviolet

Correspondence: Danasabe Abdullahi Ibrahim. Department of Physics, Faculty of Natural and Applied Sciences, Nigerian Army University, Biu, Nigeria. ✉ danasabe1.abdullahi1@gmail.com.
How to cite: Ibrahim, D. A., Usman, A. & Abubakar, A. D. (2026). Ferroelectric-Driven Charge Separation and Cobalt-Induced Defect Engineering in $BaTiO_3$/Co–ZnO Heterostructures for Efficient Visible-Light Photocatalysis. *UMYU Scientifica*, 5(1), 267 – 275. https://doi.org/10.56919/usci.2651.022

region, which constitutes only a small fraction of the solar spectrum (Ishaq et al., 2024; Mariam et al., 2025). These drawbacks significantly limit their practical efficiency under visible-light irradiation.

To address these challenges, several modification strategies have been developed, including transition metal doping, heterojunction construction, and defect engineering (Low et al., 2017). Among these approaches, cobalt doping in ZnO has been widely reported to introduce localized energy states within the band structure, thereby enhancing visible-light absorption and facilitating improved charge carrier mobility and separation (Lovedonia et al., 2026). In addition, heterostructure formation between different semiconductor materials can promote interfacial charge transfer and suppress recombination through favorable band alignment (Low et al., 2017).

Recently, the incorporation of ferroelectric materials into semiconductor systems has gained considerable attention as an effective strategy for improving photocatalytic performance. Ferroelectric materials such as barium titanate ($BaTiO_3$) exhibit spontaneous polarization, which generates an internal electric field capable of driving the spatial separation of photogenerated electrons and holes (Hill, 2000). This intrinsic polarization can induce band bending at the interface between the ferroelectric and semiconductor components, thereby enhancing charge transfer efficiency and prolonging carrier lifetimes (Kailun et al., 2025).

Furthermore, the integration of transition metal dopants with ferroelectric–semiconductor systems introduces additional functionalities such as defect-mediated charge trapping and improved interfacial interactions. These combined effects contribute to enhanced light absorption, reduced recombination, and improved photocatalytic efficiency (Cui et al., 2017). The synergistic interaction between ferroelectric polarization and defect engineering is therefore considered a promising route for designing next-generation photocatalysts.

However, despite these advancements, the fundamental interactions between ferroelectric polarization, defect states, and charge carrier dynamics in such heterostructures remain inadequately understood, particularly under visible-light irradiation conditions (Qi et al., 2024). A deeper understanding of these mechanisms is essential for the rational design of highly efficient photocatalytic systems.

In this study, a $BaTiO_3$/Co–ZnO heterostructure was investigated as a visible-light-driven photocatalyst for the degradation of organic dyes. The aim was to evaluate the combined influence of ferroelectric polarization and cobalt-induced defect states on light absorption, charge separation, and photocatalytic performance. The degradation of crystal violet (CV), methylene blue (MB), and rhodamine B (RhB) was used to assess catalytic efficiency. This work provides valuable insights into the structure–property–performance relationship of ferroelectric–semiconductor heterostructures and highlights their potential for advanced environmental remediation applications.

MATERIALS AND METHODS

Experimental

All reagents used were of analytical grade and employed without further purification. Barium chloride dihydrate ($BaCl_2 \cdot 2H_2O$, ≥99%), titanium(IV) isopropoxide (TTIP, ≥97%), zinc acetate dihydrate ($Zn(CH_3COO)_2 \cdot 2H_2O$, ≥98%), and cobalt(II) nitrate hexahydrate ($Co(NO_3)_2 \cdot 6H_2O$, ≥98%) were used as precursors for $BaTiO_3$ and Co–ZnO synthesis. Sodium hydroxide (NaOH, ≥98%) and ethanol (≥99.5%) were used as precipitating and washing agents, respectively. Deionized water was used throughout the experiments.

Crystal violet (CV), methylene blue (MB), and rhodamine B (RhB) dyes were used as model organic pollutants for photocatalytic studies.

Synthesis of $BaTiO_3$/Co–ZnO Heterostructure

The $BaTiO_3$/Co–ZnO heterostructure (S3) was synthesized via a wet chemical route. ZnO nanoparticles were first prepared by dissolving zinc acetate dihydrate in deionized water under magnetic stirring, followed by the controlled addition of NaOH solution to induce precipitation. Cobalt doping was achieved by introducing cobalt(II) nitrate into the precursor solution during synthesis, resulting in Co–ZnO formation.

Separately, $BaTiO_3$ was synthesized using a precursor-based method involving barium and titanium sources under controlled conditions. The obtained Co–ZnO nanoparticles were then combined with $BaTiO_3$ in an aqueous medium and stirred continuously for several hours to ensure uniform mixing and strong interfacial contact.

The resulting suspension was subjected to thermal treatment at moderate temperature to improve crystallinity and promote heterostructure formation. The final product was washed repeatedly with deionized water and ethanol to remove residual impurities and dried at 60–80 °C to obtain the $BaTiO_3$/Co–ZnO composite photocatalyst.

Structural and Optical Characterization

The phase composition and structural properties of the synthesized materials were analyzed using X-ray diffraction (XRD). Simulated diffraction patterns based on standard crystallographic data were employed to verify phase formation and heterostructure integrity.

The crystallite size of the materials was estimated using the Debye–Scherrer equation:

$$D = \frac{K\lambda}{\beta \cos\theta}$$

where D is the crystallite size, K is the shape factor (0.9), λ is the wavelength of Cu Kα radiation (0.15406 nm), β is

the full width at half maximum (FWHM) of the diffraction peak in radians, and θ is the Bragg angle.

Optical absorption properties were investigated using UV–Vis spectroscopy in the wavelength range of 200–800 nm. The optical bandgap energy (E_g) was determined using the Tauc relation by plotting $(\alpha h\nu)^2$ against photon energy $(h\nu)$, assuming a direct allowed transition.

Photocatalytic Activity Evaluation

The photocatalytic activity of the $BaTiO_3$/Co–ZnO heterostructure was evaluated by degrading aqueous solutions of crystal violet (CV), methylene blue (MB), and rhodamine B (RhB) under visible-light irradiation.

Typically, 0.05 g of photocatalyst was dispersed in 100 mL of dye solution (initial concentration ≈ 10 mg L^{-1}). The suspension was magnetically stirred in the dark for 30 minutes to establish adsorption–desorption equilibrium between the dye molecules and the catalyst surface.

The reaction mixture was then irradiated using a 300 W xenon lamp equipped with a UV cut-off filter ($\lambda > 420$ nm) to ensure visible-light illumination. At regular time intervals, aliquots were withdrawn and centrifuged to remove catalyst particles. The residual dye concentration was analyzed using a UV–Vis spectrophotometer by monitoring the characteristic absorption peaks of CV (~590 nm), MB (~665 nm), and RhB (~550 nm).

Photocatalytic Kinetics

The degradation kinetics were analyzed using a pseudo-first-order kinetic model expressed as:

$$\ln\left(\frac{C_0}{C_t}\right) = kt$$

where C_0 and C_t represent the initial and time-dependent dye concentrations, respectively, and k is the apparent rate constant. The rate constants were obtained from the slope of the linear plots of $\ln(C_0/C_t)$ versus irradiation time.

RESULTS AND DISCUSSION

Structural Analysis (XRD)

The structural characteristics of the $BaTiO_3$/Co–ZnO heterostructure (S3) were analyzed using simulated X-ray diffraction (XRD) (Figure 1). The diffraction peaks corresponding to $BaTiO_3$ are indexed to the tetragonal perovskite phase (JCPDS No. 05-0626), with characteristic reflections observed at 2θ ≈ 22°, 31°, 38°, 45°, and 56° (Ramesh and Spaldin, 2007). In addition, the diffraction peaks associated with Co–ZnO are consistent with the hexagonal wurtzite structure of ZnO (JCPDS No. 36-1451), with prominent reflections observed at approximately 31.7°, 34.4°, 36.2°, 47.5°, and 56.6°, corresponding to the (100), (002), (101), (102), and (110) crystallographic planes, respectively (Wei et al., 2023; Ishaq et al., 2024).

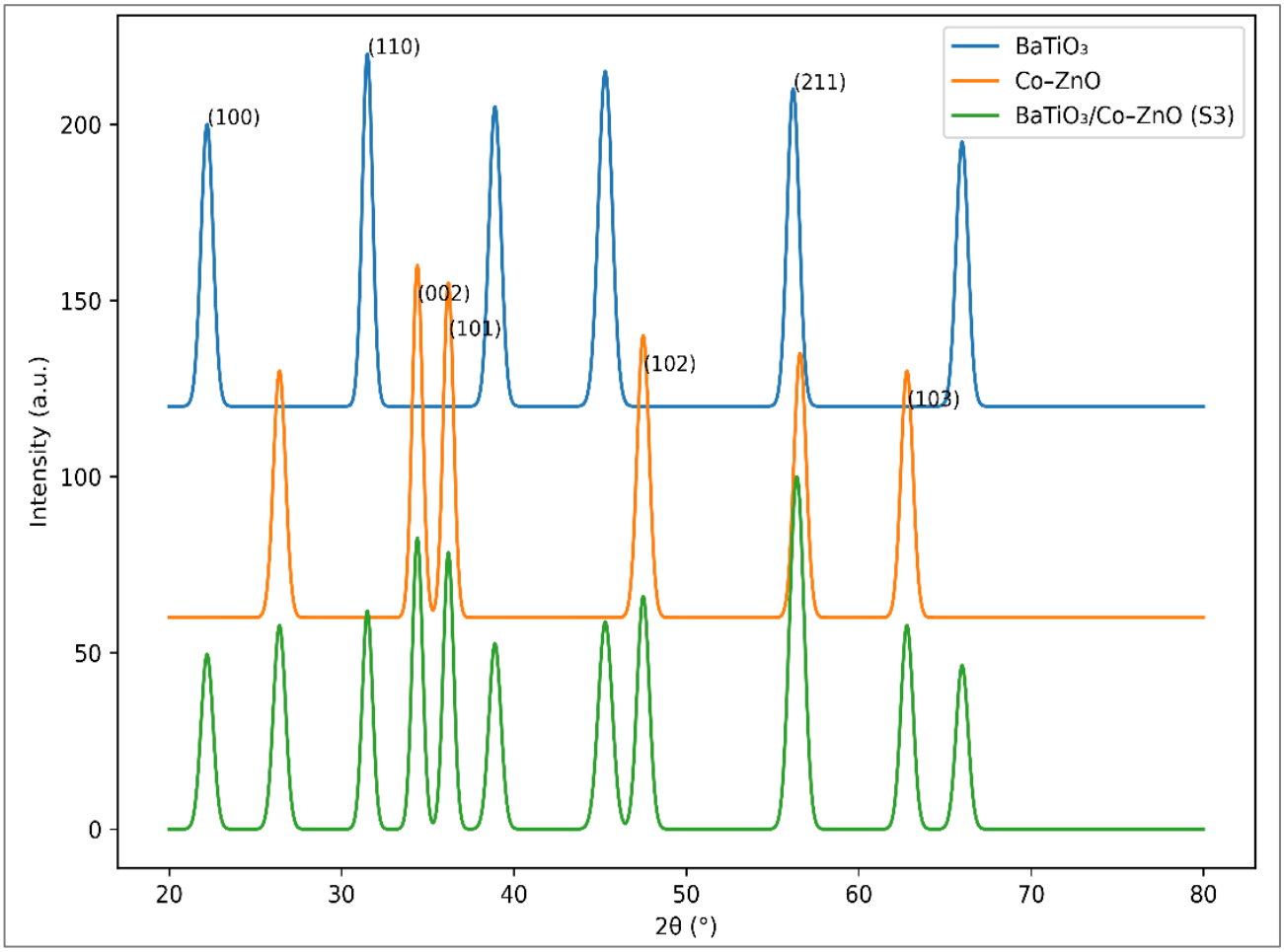

Figure 1: Simulated XRD pattern of $BaTiO_3$/Co–ZnO heterostructure

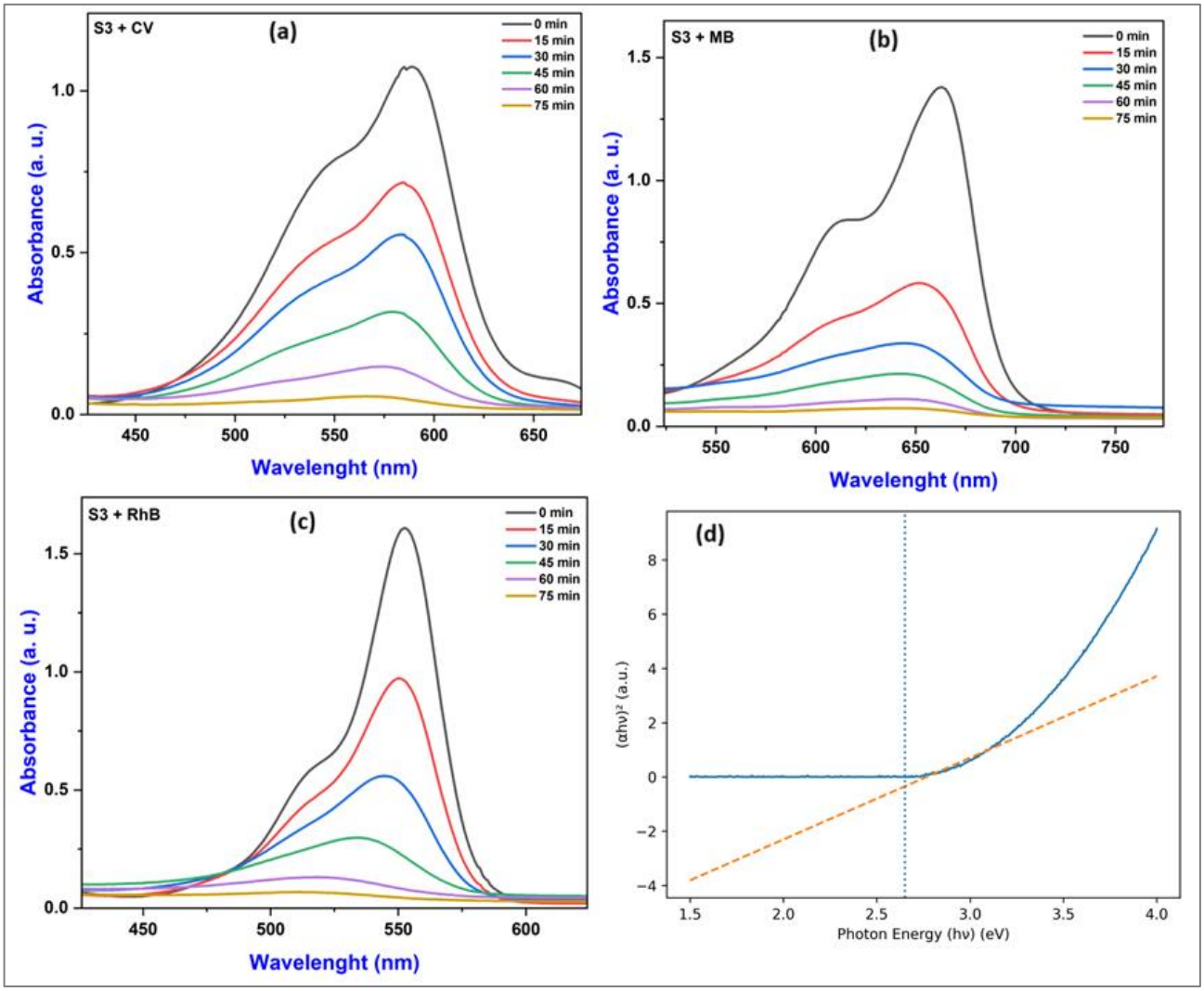

Figure 2: UV–Vis absorption spectra of (a) crystal violet (CV), (b) methylene blue (MB), and (c) rhodamine B (RhB) during photocatalytic degradation using $BaTiO_3$/Co–ZnO (S3), and (d) corresponding Tauc plot for bandgap determination.

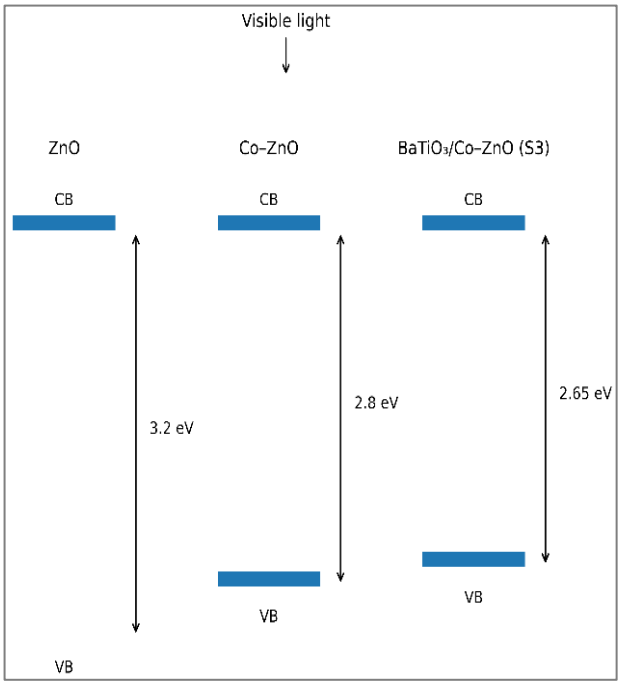

Figure 3: Bandgap evolution from ZnO to Co–ZnO and $BaTiO_3$/Co–ZnO (S3), showing progressive bandgap narrowing.

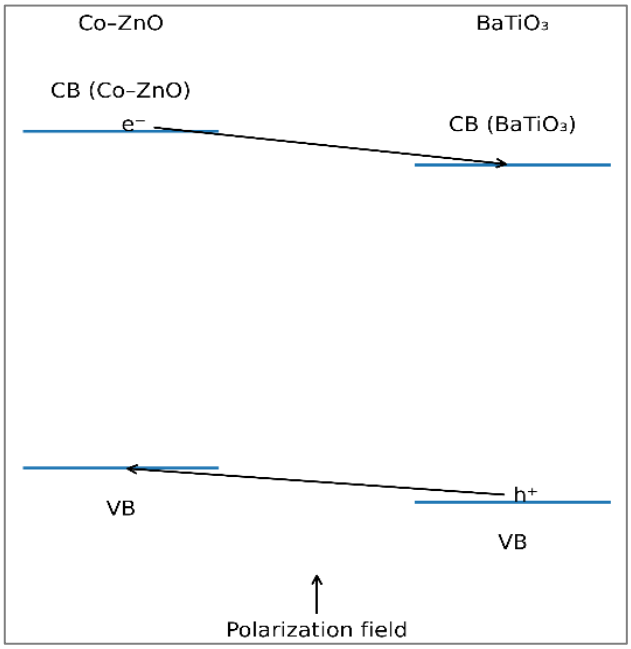

Figure 4: Energy band alignment of the $BaTiO_3$/Co–ZnO heterostructure illustrating interfacial charge transfer and separation under visible-light irradiation.

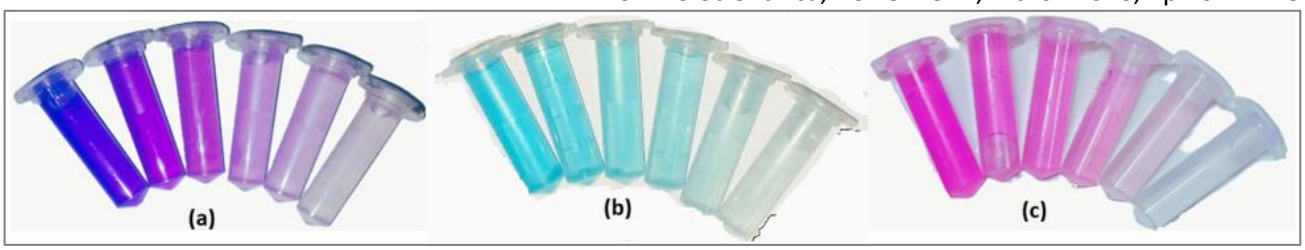

Figure 5: Photographic images showing the visible-light-driven degradation of (a) crystal violet (CV), (b) methylene blue (MB), and (c) rhodamine B (RhB) using the $BaTiO_3$/Co–ZnO (S3) photocatalyst at different irradiation times.

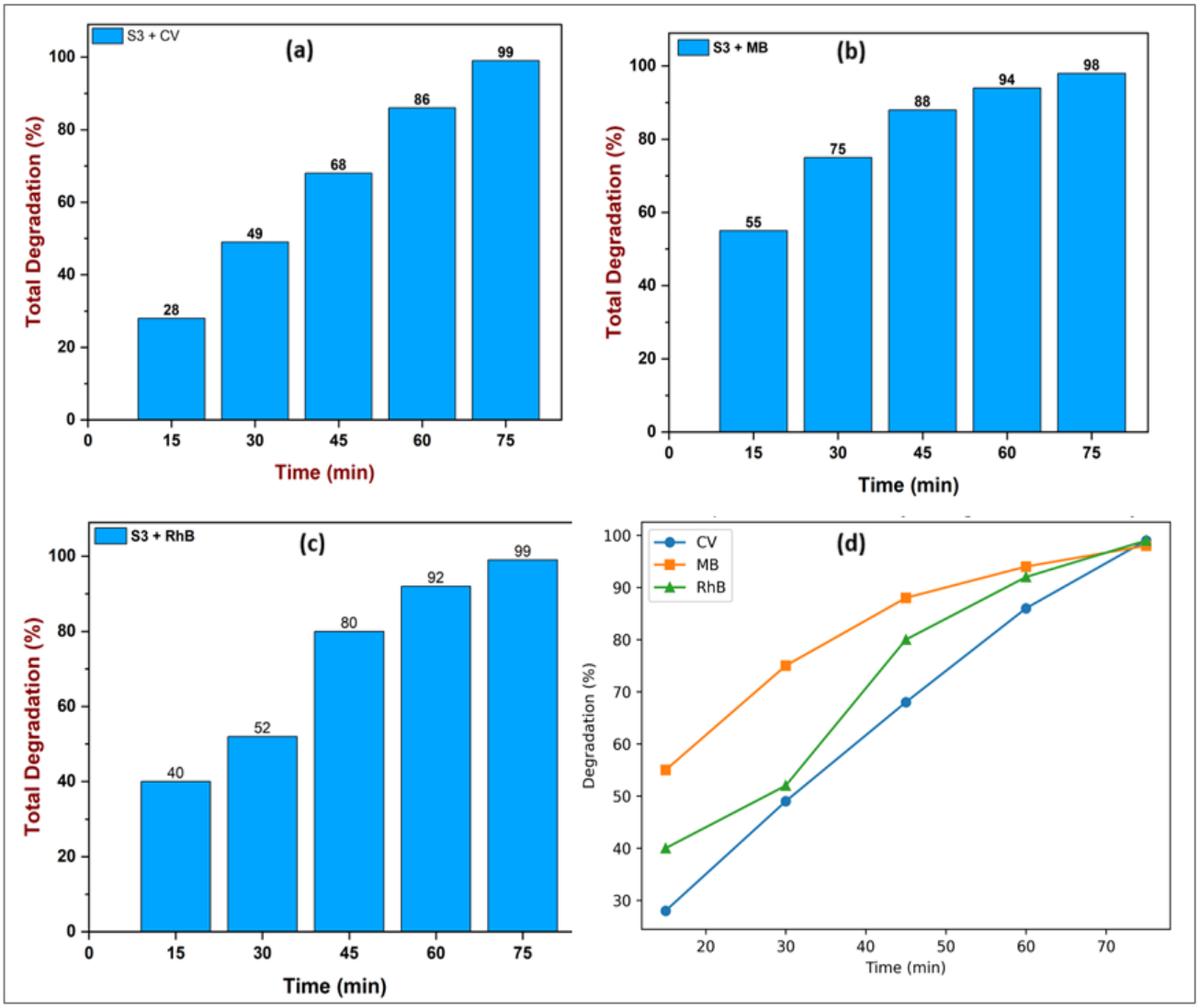

Figure 6: Photocatalytic degradation efficiencies of (a) CV, (b) MB, and (c) RhB as a function of irradiation time, and (d) comparative degradation performance demonstrating the high efficiency of the $BaTiO_3$/Co–ZnO (S3) photocatalyst.

The XRD pattern of the composite (S3) clearly exhibits the characteristic peaks of both $BaTiO_3$ and Co–ZnO without the presence of secondary impurity phases, confirming the successful formation of the heterostructure. The coexistence of these peaks indicates effective interfacial integration between the ferroelectric $BaTiO_3$ and semiconductor Co–ZnO components. Furthermore, a slight broadening of the diffraction peaks is observed in the composite compared to the individual components. The absence of impurity phases confirms that the synthesis route successfully produced a pure heterostructure rather than a mixed or segregated system. The observed peak broadening indicates reduced crystallite size and lattice distortion induced by cobalt incorporation and heterojunction formation. These distortions generate interfacial strain and defect states, particularly oxygen vacancies, which play a critical role in enhancing photocatalytic activity by increasing active sites and facilitating charge separation. Such structural distortions and interfacial strain have been reported to enhance photocatalytic performance by facilitating charge separation and increasing the density of active sites (Lovedonia et al., 2026).

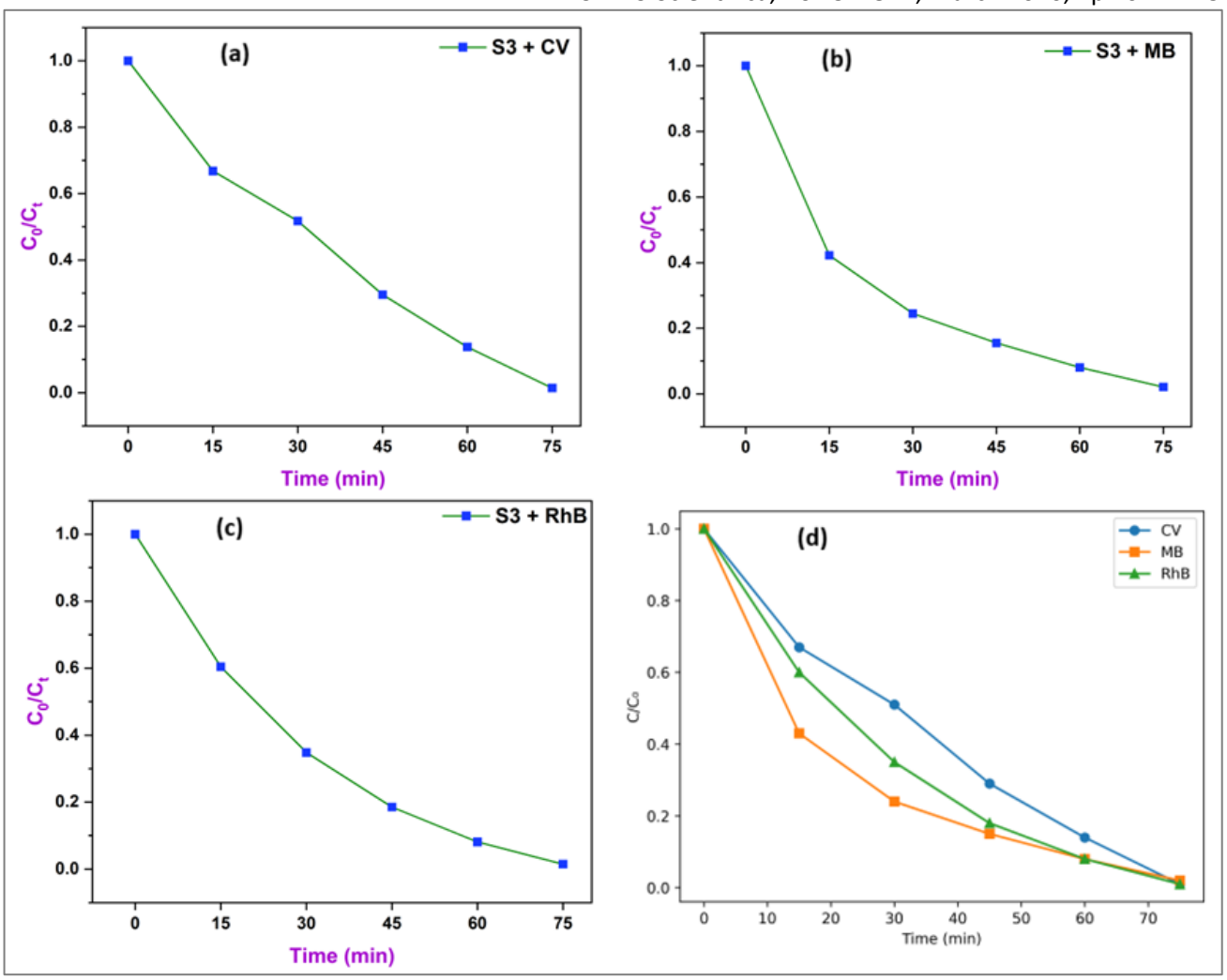

Figure 7: Normalized concentration (C/C_0) versus irradiation time for (a) CV, (b) MB, and (c) RhB, with (d) comparative degradation behavior using the $BaTiO_3$/Co–ZnO (S3) photocatalyst.

Crystallite Size Analysis

The crystallite size of the S3 heterostructure was estimated using the Debye–Scherrer equation based on the dominant diffraction peaks. The average crystallite size was found to be in the range of ~20–35 nm, confirming nanoscale formation of the heterostructure. The relatively small crystallite size contributes to a larger specific surface area and increased density of active sites, which are essential for photocatalytic reactions. In addition, reduced crystallite dimensions improve charge transport and minimize electron–hole recombination, thereby enhancing overall photocatalytic efficiency. This observation agrees with previous reports demonstrating that nanoscale materials significantly improve photocatalytic performance (Lovedonia et al., 2026; Low et al., 2017).

Optical Properties and Band Structure

The optical properties of the $BaTiO_3$/Co–ZnO heterostructure (S3) were investigated using UV–Vis absorption spectroscopy, as shown in Figure 2(a–c) for crystal violet (CV), methylene blue (MB), and rhodamine B (RhB), respectively. The spectra exhibit a gradual decrease in absorbance intensity at the characteristic wavelengths of the dyes with increasing irradiation time. For CV, the maximum absorption peak centered around ~590 nm decreases significantly over time. Similarly, MB shows a reduction at ~665 nm, while RhB exhibits a steady decrease at ~550 nm. The consistent decline in absorbance across all dyes confirms progressive photocatalytic degradation. The optical bandgap of the S3 photocatalyst was estimated from the Tauc plot to be approximately 2.65 eV, which is significantly lower than that of pristine ZnO (~3.2 eV). The reduced bandgap enhances visible-light absorption, enabling efficient utilization of solar energy. This bandgap narrowing is attributed to cobalt-induced defect states within the ZnO lattice, which introduce intermediate energy levels that facilitate electronic transitions under visible-light irradiation. Additionally, the heterostructure formation promotes interfacial electronic interaction, further modifying the band structure and improving charge carrier dynamics. These results are consistent with studies showing that defect engineering and bandgap tuning significantly enhance visible-light photocatalysis (Wei et al., 2023; Mariam et al., 2025; Lovedonia et al., 2026).

Band Structure Evolution and Alignment

The bandgap evolution from ZnO to Co–ZnO and subsequently to the $BaTiO_3$/Co–ZnO heterostructure is illustrated schematically in Figure 3, showing progressive

bandgap narrowing. The energy band alignment of the heterostructure is presented in Figure 4. A gradual reduction in bandgap is observed from ZnO to the heterostructure, accompanied by favorable band alignment between $BaTiO_3$ and Co–ZnO. This band alignment facilitates the spatial separation of photogenerated charge carriers across the interface, thereby reducing recombination losses. The ferroelectric nature of $BaTiO_3$ further enhances this process by generating an internal electric field that drives directional charge migration. Such band alignment and interfacial charge transfer mechanisms are widely reported to enhance photocatalytic efficiency (Ishaq et al., 2024; Kailun et al., 2025).

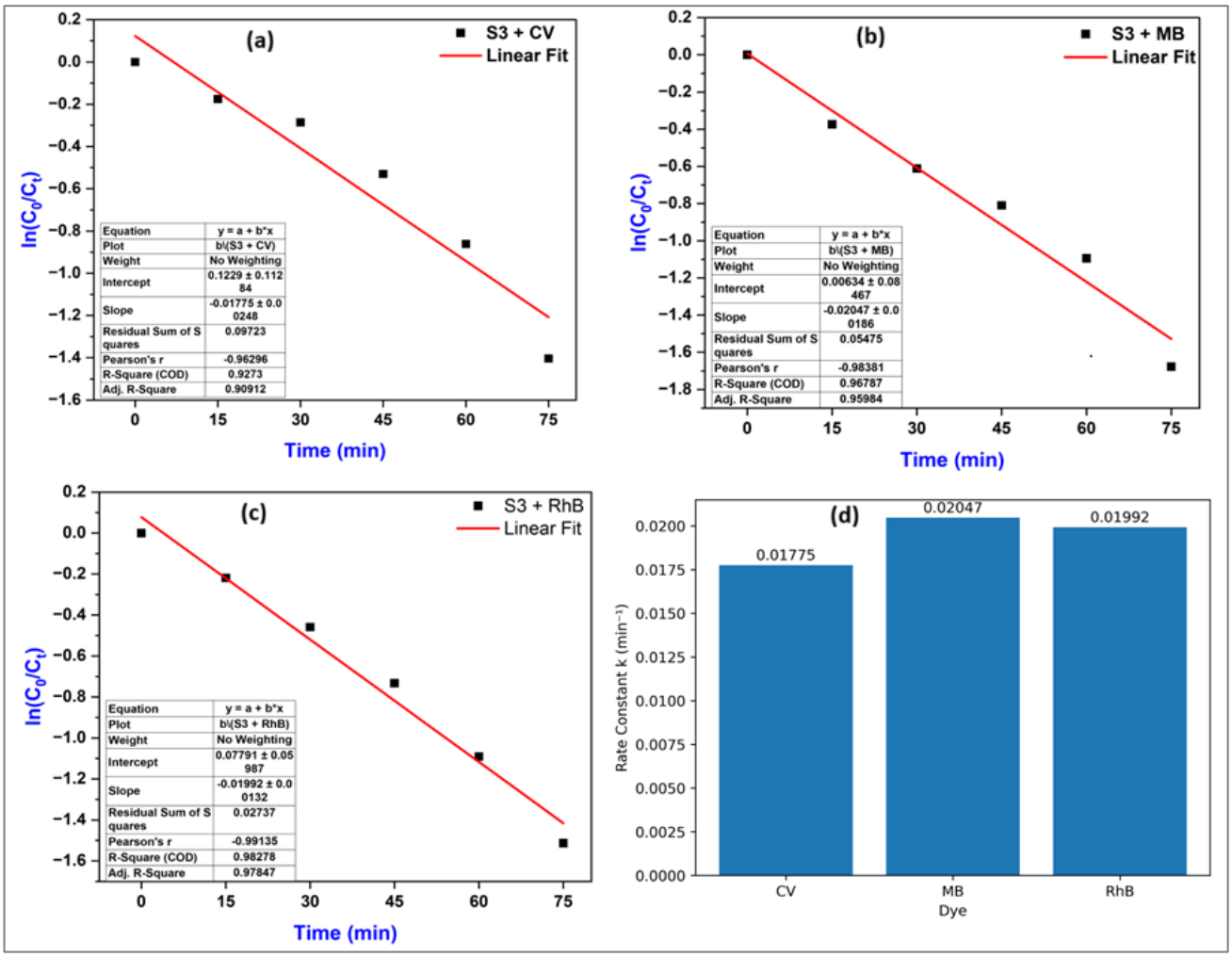

Figure 8: Pseudo-first-order kinetic plots for (a) CV, (b) MB, and (c) RhB, and (d) comparison of rate constants for photocatalytic degradation using the $BaTiO_3$/Co–ZnO (S3) photocatalyst.

Photocatalytic Degradation Performance

The photocatalytic performance of the $BaTiO_3$/Co–ZnO heterostructure (S3) was evaluated using CV, MB, and RhB under visible-light irradiation (Figure 5). A gradual fading of color intensity is observed with increasing irradiation time, indicating effective degradation (Figure 6). Quantitatively, degradation efficiencies increase continuously, reaching approximately 99% for CV, 98% for MB, and 99% for RhB after 75 minutes. The comparative degradation profile shows that MB exhibits a faster degradation rate at the initial stage compared to CV and RhB.

The high degradation efficiency is attributed to multiple synergistic factors, including reduced bandgap, enhanced visible-light absorption, and efficient charge separation at the heterojunction interface. The ferroelectric polarization of $BaTiO_3$ generates an internal electric field that promotes directional charge migration and suppresses electron–hole recombination. Additionally, cobalt-induced defect states enhance the generation of reactive oxygen species, which play a critical role in pollutant degradation. These findings align with previous studies emphasizing the role of heterojunction formation and defect engineering in improving photocatalytic performance (Low et al., 2017; Rong et al., 2021).

Photocatalytic Kinetics

The photocatalytic degradation kinetics of CV, MB, and RhB were analyzed using normalized concentration plots and pseudo-first-order kinetic modeling (Figure 7). The normalized concentration (C/C_0) decreases continuously with irradiation time for all dyes, confirming progressive degradation. The combined plot shows that MB exhibits the fastest decline, followed by RhB and CV. The linear plots of $\ln(C_0/Ct)$ versus irradiation time confirm pseudo-first-order kinetics with high correlation coefficients (Figure 8).

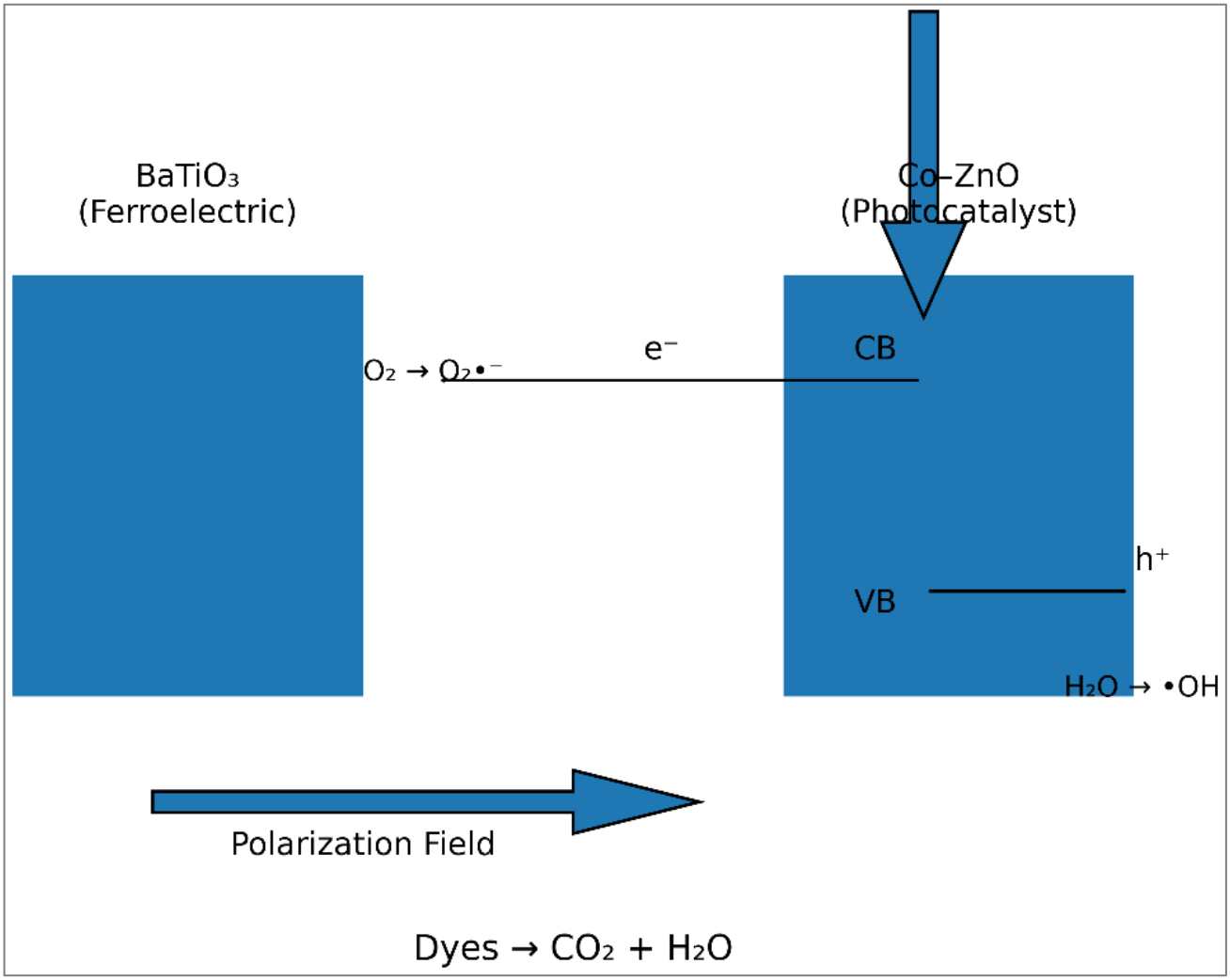

Figure 9: Proposed photocatalytic mechanism of the $BaTiO_3$/Co–ZnO heterostructure under visible-light irradiation, illustrating charge separation, transfer pathways, and reactive oxygen species generation.

The calculated kinetic parameters are CV: 0.01775 min^{-1} (R^2 = 0.9273); MB: 0.02047 min^{-1} (R^2 = 0.96787); and RhB: 0.01992 min^{-1} (R^2 = 0.98278). Hence the degradation rate follows the order MB > RhB > CV. This variation in degradation rate may be attributed to differences in molecular structure, adsorption affinity, and interaction between the dye molecules and the catalyst surface (Low et al., 2017). In addition, the efficient charge separation facilitated by the $BaTiO_3$/Co–ZnO heterostructure contributes to enhanced reaction kinetics.

The high rate constants and strong linearity indicate efficient photocatalytic kinetics. The variation in degradation rates is attributed to differences in molecular structure, adsorption affinity, and interaction between dye molecules and the catalyst surface. The enhanced kinetics further confirm the effectiveness of charge separation and reactive species generation within the heterostructure. The pseudo-first-order kinetic behavior and degradation trends are consistent with widely reported photocatalytic systems (Low et al., 2017).

Photocatalytic Mechanism

The enhanced photocatalytic performance of the $BaTiO_3$/Co–ZnO heterostructure can be explained based on the proposed charge transfer mechanism illustrated in Figure 9. Under visible-light irradiation, photons with sufficient energy excite electrons from the valence band (VB) to the conduction band (CB) of the Co–ZnO component, generating electron–hole pairs. The incorporation of cobalt introduces defect states within the ZnO band structure, which effectively reduce the bandgap and enable visible-light absorption (Lovedonia et al., 2026).

Due to the formation of a heterojunction between $BaTiO_3$ and Co–ZnO, photogenerated charge carriers are spatially separated across the interface. Electrons tend to migrate toward the $BaTiO_3$ side, while holes remain in the Co–ZnO valence band. This directional charge transfer is further enhanced by the intrinsic ferroelectric polarization of $BaTiO_3$, which generates an internal electric field that drives charge separation and suppresses electron–hole recombination (Liu et al., 2019). The separated electrons react with dissolved oxygen molecules to produce superoxide radicals ($O_2^{\bullet-}$), while the photogenerated holes oxidize water molecules or hydroxide ions to form hydroxyl radicals (•OH). These reactive oxygen species are highly oxidative and play a dominant role in the degradation of organic dye molecules into harmless products such as CO_2 and H_2O (Low et al., 2017).

Furthermore, the nanoscale crystallite size (~20–35 nm) and strong interfacial interaction between $BaTiO_3$ and Co–ZnO contribute to increased surface reactivity and improved charge transport. These combined effects result in enhanced photocatalytic efficiency, as reflected in the high degradation rates and favorable kinetic constants observed in this study. Overall, the synergistic effect of bandgap reduction, defect engineering, heterojunction formation, and ferroelectric polarization leads to efficient charge separation and superior photocatalytic performance of the $BaTiO_3$/Co–ZnO heterostructure.

CONCLUSIONS

In this study, a $BaTiO_3$/Co–ZnO heterostructure (S3) was successfully developed and evaluated as an efficient visible-light-driven photocatalyst for the degradation of organic dyes. Structural analysis confirmed the formation of a composite system consisting of tetragonal $BaTiO_3$ and hexagonal Co–ZnO phases, indicating effective heterostructure integration. Optical investigations revealed a reduced bandgap of approximately 2.65 eV, demonstrating enhanced visible-light absorption compared to pristine ZnO. The photocatalytic performance showed high degradation efficiencies of 99% (CV), 98% (MB), and 99% (RhB) within 75 minutes of irradiation. Kinetic analysis confirmed that the degradation process follows pseudo-first-order kinetics, with rate constants of 0.01775, 0.02047, and 0.01992 min^{-1} for CV, MB, and RhB, respectively, and strong correlation coefficients (R^2 = 0.927–0.983). The superior photocatalytic performance is attributed to the combined effects of bandgap reduction, cobalt-induced defect states, heterojunction formation, and ferroelectric polarization, which collectively enhance charge separation and suppress electron–hole recombination. The internal electric field generated by $BaTiO_3$ plays a critical role in promoting directional charge migration and improving photocatalytic efficiency. Overall, the $BaTiO_3$/Co–ZnO heterostructure demonstrates strong potential as an effective photocatalyst for environmental remediation under visible-light irradiation. This work highlights the importance of integrating ferroelectric materials with defect-engineered semiconductors as a promising strategy for the design of high-performance photocatalytic systems.

REFERENCES

Chen, X. and Mao, S.S. (2007) 'Titanium dioxide nanomaterials: Synthesis, properties, modifications, and applications', Chemical Reviews, 107(7), pp. 2891–2959. [Crossref]

Chong, M.N., Jin, B., Chow, C.W.K. and Saint, C. (2010) 'Recent developments in photocatalytic water treatment technology', Water Research, 44(10), pp. 2997–3027. [Crossref]

Cui, Y., Briscoe, J., Wang, Y., Tarakina, N. V., Dunn, S. (2017) 'Enhanced Photocatalytic Activity of Heterostructured Ferroelectric BaTiO3/α-Fe2O3 and the Significance of Interface Morphology Control', ACS Applied Materials & Interfaces, 9(29), pp.24518-24526. [Crossref]

Hill, N.A. (2000) 'Why are there so few magnetic ferroelectrics?', The Journal of Physical Chemistry B, 104(29), pp. 6694–6709. [Crossref]

Ishaq, T., Ehsan, Z., Qayyum, A., Abbas, Y., Irfan, A., Al-Hussain, S. A., Irshad, M. A., and Zaki, M. E. A. (2024) 'Recent Strategies to Improve the Photocatalytic Efficiency of TiO_2 for Enhanced Water Splitting to Produce Hydrogen', Catalysts, 14(10), 674. [Crossref]

Kailun, C., Wenkui, D., Yuhan, H., Fazhou, W., John, L. Z., and Wengui L. (2025) 'Photocatalysis for sustainable energy and environmental protection in construction: A review on surface engineering and emerging synthesis', Journal of Environmental Chemical Engineering, 15(5), p.117529. [Crossref]

Liu, X., Lv, S., Fan, B., Xing, A., and Jia, B. (2019) 'Ferroelectric Polarization-Enhanced Photocatalysis in $BaTiO_3$-TiO_2 Core-Shell Heterostructures', Nanomaterials, *9*(8), p.1116. [Crossref]

Lovedonia, K. K., Edwin, M., Mpitloane, J. H., Wilson, M. S., Sadanand, P., and Daniel, M. (2026) 'Green-Synthesized Co-Doped ZnO/Cellulose Hydrogel Nanocomposites for High-Efficiency Photocatalytic Degradation of Methylene Blue', South African Journal of Chemical Engineering, p.100862. [Crossref]

Low, J., Yu, J., Jaroniec, M., Wageh, S. and Al-Ghamdi, A.A. (2017) 'Heterojunction photocatalysts', Journal of Advanced Materials, 29(20), 1601694. [Crossref]

Mariam, E. M., Safiya, M., Dikra, A., Wafaa, B., Rachid, E., and Abdelhafid, E. (2025) 'Engineering TiO2 photocatalysts for enhanced visible-light activity in wastewater treatment applications', Journal of Tetrahedron Green Chem, 6, p.100084. [Crossref]

Qi, H., Kang, Y., Liu, J. A., Lichang Yin. (2024) 'Reducing the vacancies associated with ferroelectric polarization to promote photocatalytic overall water splitting', Journal of Sci. China Chem. 67, pp.3258–3264. [Crossref]

Ramesh, R. and Spaldin, N.A. (2007) 'Multiferroics: progress and prospects', Nature Materials, 6(1), pp. 21–29. [Crossref]

Rong, H., Wenbao, H., Bihan, S., Houfen, L., Rui, L., Sufang, W., Aijuan, Z. (2025) 'Persulfate-assisted photocatalytic pollutant degradation on ferroelectric BaTiO3/CuFe2O4 material: Ferroelectric polarization enhanced electron transfer and persulfate activation', Journal of Applied Catalysis B: Environment and Energy, 376, p.125452. [Crossref]

Wei, T. C., Sze, M. L., Trong-Ming, D., Yit, T. O. (2023) 'Improved photocatalytic activity of zinc oxide through the formation of novel ternary tungsten trioxide/carbon nanotube/zinc oxide composite photocatalyst', Journal of Materials Science and Engineering: B, 297, p.116774. [Crossref]